3768 *Chem. Mater.* **2010,** *22,* 3768–3772
DOI:10.1021/cm100810g

CHEMISTRY OF MATERIALS
Article

One-Pot Biofunctionalization of Magnetic Nanoparticles via Thiol−Ene Click Reaction for Magnetic Hyperthermia and Magnetic Resonance Imaging

Koichiro Hayashi,[†] Kenji Ono,[‡] Hiromi Suzuki,[‡] Makoto Sawada,[‡] Makoto Moriya,[†] Wataru Sakamoto,[†] and Toshinobu Yogo*,[†]

[†]*Division of Nanomaterials Science, EcoTopia Science Institute, Nagoya University, Furo-cho, Chikusa-ku, Nagoya 464-8603, Japan, and* [‡]*Department of Brain Function, Research Institute of Environmental Medicine, Nagoya University, Furo-cho, Chikusa-ku, Nagoya 464-8601, Japan*

Received March 22, 2010. Revised Manuscript Received May 3, 2010

Cysteine-modified Fe_3O_4 nanoparticles (Cys-Fe_3O_4 NPs) were synthesized by the one-pot biofunctionalization of allyl-functionalized Fe_3O_4 NPs (allyl-Fe_3O_4) with cysteine using the *in situ* hydrolysis−condensation of iron(III) allylacetylacetonate and the thiol−ene click reaction. The particle size of Fe_3O_4 in Cys-Fe_3O_4 NPs measured by transmission electron microscopy and X-ray diffraction analysis was ∼8 nm. Cys-Fe_3O_4 NPs were soluble in water and had a hydrodynamic diameter of 22 nm and prolonged stability in water. They were superparamagnetic, which was confirmed by fitting the Langevin equation to the magnetization data, generated heat in an alternating current (AC) magnetic field, and had a specific absorption rate (SAR) of 156 W g^{-1} at 230 kHz and 100 Oe. In addition, they exhibited a T_2-weighted magnetic resonance imaging (MRI) contrast-enhancing effect.

Introduction

Magnetic nanoparticles (MNPs) have attracted attention because of their potential application in magnetic hyperthermia,[1,2] drug delivery,[3,4] magnetic resonance imaging (MRI),[5−7] and fluid transport.[8] MNPs for such biomedical applications should be hydrophilic and biocompatible. MNPs with these properties can be realized by modifying the MNPs with biomolecules such as amino acids, peptides, and antibodies. A conventional strategy for biomolecule modification is the formation of amide bonds by a condensation reaction between amino groups on surface of MNPs and the carboxylic groups of biomolecules.[9] The reaction entails the protection and deprotection of unnecessary functional groups to prevent unintended bond formation and therefore is a multistep complex reaction. These problems can be solved by the application of click chemistry.[10]

Click chemistry is a simple, chemoselective, and high-yield reaction. Furthermore, the reaction effectively proceeds under any environment, including underwater conditions, and can bind any compound with another. Radical addition of thiol to alkene, the thiol−ene reaction, is a click reaction and is widely employed in the field of polymers.[11] Although the thiol−ene click reaction is quite useful, there is no report on the modification of MNPs with organic compounds via this reaction. This is attributed to the difficulty in synthesizing the carbon−carbon double bond-immobilized MNPs because the bond undergoes polymerization during high-temperature heat treatment. For example, the thermal decomposition of metal-containing precursors, a representative synthetic method for MNPs, requires high-temperature treatment, above 300 °C, to yield MNPs.[12]

We have successfully synthesized allyl (CH_2=$CHCH_2$)-functionalized MNPs through *in situ* hydrolysis−condensation of iron(III) 3-allylacetylacetonate (IAA) at low temperature (∼80 °C).[13] In this reaction process, the allyl group does not undergo polymerization like the vinyl group, and hence, it is stable to heat. Moreover, the group has the

*To whom correspondence should be addressed. E-mail: yogo@esi.nagoya-u.ac.jp.

(1) Mornet, S.; Vasseur, S.; Grasset, F.; Duguet, E. *J. Mater. Chem.* **2004**, *14*, 2161.
(2) Day, E. S.; Morton, J. G.; West, J. L. *J. Biomech. Eng. Trans. ASME* **2009**, *131*, 074001.
(3) Arruebo, M.; Fernández-Pacheco, R.; Ibarra, M. R.; Santamaria, J. *Nano Today* **2007**, *2*, 22.
(4) Duran, J. D. G.; Arias, J. L.; Gallardo, V.; Delgado, A. V. J. *Pharmaceutical Sci.* **2008**, *97*, 2948.
(5) Gazeau, F.; Levy, M.; Wilhelm, C. *Nanomedicine* **2008**, *3*, 831.
(6) Corot, C.; Robert, P.; Idée, J.-M.; Port, M. *Adv. Drug Delivery Rev.* **2006**, *58*, 1471.
(7) Goya, G. F.; Grazu, V.; Ibarra, M. R. *Curr. Nanosci.* **2008**, *4*, 1.
(8) Latham, A. H; Williams, M. E. *Acc. Chem. Res.* **2008**, *41*, 411.
(9) Kohler, N.; Fryxell, G. E.; Zhang, M. *J. Am. Chem. Soc.* **2004**, *126*, 7206.
(10) Kolb, H. C.; Finn, M. G.; Sharpless, K. B. *Angew. Chem., Int. Ed.* **2001**, *40*, 2004.
(11) Dondoni, A. *Angew. Chem., Int. Ed.* **2008**, *47*, 8995.
(12) Sun, S.; Zeng, H. *J. Am. Chem. Soc.* **2002**, *124*, 8204.
(13) Hayashi, K.; Shimizu, T.; Asano, H.; Sakamoto, W.; Yogo, T. *J. Mater. Res.* **2008**, *23*, 3415.

Published on Web 05/13/2010

advantage of being unreactive with other functional groups except under particular reaction conditions. On the basis of the thermal and chemical stability of the allyl group, we have modified the MNPs with folic acid. However, the modification procedure involves multiple steps and is complex.[14]

A typical magnetic material for biomedical application includes magnetite (Fe_3O_4). Fe_3O_4 is nontoxic and stable in water and air, and has relatively high saturation magnetization. In contrast, iron NPs are easily oxidized, although they have extremely high saturation magnetization. In addition, the saturation magnetization of Fe_3O_4 is higher than that of other ferrites (MFe_2O_4; M = Mg, Co, Ni, Zn, Cu, Li, etc.).[15] Therefore, Fe_3O_4 is the optimum material for magnetic diagnosis and treatment of humans.

As superparamagnetic NPs generate heat under an alternating current (AC) magnetic field by Néel relaxation, they are applicable to heating devices for cancer thermotherapy or magnetic hyperthermia. It is known that the cell survival rate decreases gradually up to 42 °C and decreases abruptly above this temperature.[16] Therefore, the localization of superparamagnetic NPs to tumors and the application of an AC magnetic field allow the selective destruction of tumor cells. Generally, the usable range of amplitudes (H) and frequencies (f) is considered to be H = 0−200 Oe and f = 0.05−1.2 MHz.[17] In addition, the appropriate concentration of MNPs in each cubic centimeter of tumor tissue is reasonably assumed to be 5−10 mg in human patients.[17]

In addition, superparamagnetic NPs can decrease T_2 or the transverse relaxation time to enhance MRI contrast.[18] Examples of MRI contrast agents using superparamagnetic iron oxide NPs include Resovist, Endorem, and Feridex, which are used for liver imaging.[19]

This article describes the one-pot biofunctionalization of NPs via the thiol−ene click reaction using *in situ* synthesized allyl-functionalized Fe_3O_4 nanoparticles (allyl-Fe_3O_4 NPs) and cysteine. Cysteine, a water-soluble and sulfur-containing amino acid, was selected to make the NPs hydrophilic and biocompatibile. Furthermore, the exothermic properties and MRI contrast-enhancing effect of the NPs were characterized.

Experimental Section

Materials. IAA was prepared by a method described in the literature.[20] Ethanol (Kishida Chemical, Japan) was dried over magnesium ethoxide and then distilled before use. Azobisisobutyronitrile (AIBN) was recrystallized from methanol. The following materials were used as received: hydrazine monohydrate ($N_2H_4 \cdot H_2O$, Tokyo Kasei, Japan) and L-cysteine (Sigma-Aldrich, USA).

Synthesis of Allyl-Functionalized Fe_3O_4 Nanoparticles (Allyl-Fe_3O_4 NPs). IAA (1.0 g, 2.1 mmol) was dissolved in ethanol (30 mL). H_2O (1.36 g, 75.6 mmol) and $N_2H_4 \cdot H_2O$ (0.42 g, 8.4 mmol), the accelerant and reducing agent, respectively, were added to the precursor solution at room temperature. The reaction mixture was then refluxed at ~80 °C for 24 h to yield an allyl-Fe_3O_4 NP-dispersed ethanol solution. The solution was cooled to room temperature.

Synthesis of Cysteine-Functionalized Fe_3O_4 Nanoparticles (Cys-Fe_3O_4 NPs). A cysteine (254 mg, 2.1 mmol)−water solution (10 mL) and AIBN (10 mg, 6.3×10^{-2} mmol)−ethanol solution (10 mL) were added to the as-prepared allyl-Fe_3O_4 NP-dispersed ethanol solution at room temperature. The mixture solution was heated at 60 °C for 1 h to modify Fe_3O_4 NPs with cysteine via the thiol−ene click reaction, the reaction between the thiol group of cysteine and the allyl group on the surface of Fe_3O_4 NPs. Subsequently, Cys-Fe_3O_4 NPs were collected by centrifugation and washed with water several times.

Structural Analysis. The IR spectra of IAA, allyl-Fe_3O_4 NPs, Cys-Fe_3O_4 NPs, and cysteine were analyzed using a FTIR spectrometer (Nicolet, Nexus 470, Madison, WI). The organic components of Cys-Fe_3O_4 NPs were measured by differential thermal analysis−thermogravimetry (DTA-TG, Rigaku, TG8120, Tokyo, Japan). The crystalline phases in Cys-Fe_3O_4 NPs were analyzed by X-ray diffraction (XRD) using CuKα radiation with a monochromator (Rigaku, RINT-2500). The crystallite size was estimated using the 311 reflection of Fe_3O_4 on the basis of the Scherrer equation. Cys-Fe_3O_4 NPs were observed by transmission electron microscopy (TEM, Hitachi, H-800). The hydrodynamic diameter of Cys-Fe_3O_4 NPs was measured by dynamic light scattering (DLS, Nikkiso, UPA-150). The mass spectrometry of Cys-Fe_3O_4 NPs was performed by matrix-assisted laser desorption/ionization mass spectrometry (MALDI-MS, Bruker, Ultraflex III) using α-cyano-4-hydroxycinnamic acid (CHCA) as the organic matrix.[21]

Magnetic Properties. The magnetic property of the product was measured with a superconducting quantum interference device (SQUID, Quantum Design, MPMS-7, San Diego, CA).

Hyperthermia Experiment. The hyperthermia experiment using Cys-Fe_3O_4 NPs was performed by a method similar to a previously reported method.[13] To evaluate the heating properties of the product, an agar phantom dispersed with Cys-Fe_3O_4 NPs was subjected to an AC magnetic field with a frequency of 230 kHz and an amplitude of 100 Oe, which were generated using a transistor inverter with field coils (ϕ 120 mm × 5 turns). This agar phantom, used as simulated tissues, was spherical (ϕ = 20 mm) and consisted of agar (4%), sodium chloride (0.24%), sodium azide (0.1%), and water (95.66%). The mass of Cys-Fe_3O_4 NPs in a milliliter of the agar phantom was 10 mg. The temperature of the agar phantom was measured as a function of time using a platinel thermocouple directly inserted into the phantom under an AC magnetic field.

Cytotoxicity Assay. Glioma (GL) 261 cells were seeded at 5×10^5 cells in a plastic dish with a medium. Cys-Fe_3O_4 NPs (100 μg mL^{-1}) were added to the dish. The cytotoxicity of Cys-Fe_3O_4 NPs was evaluated by determining the viability of the cells after incubating them for 24 h.

***In Vitro* MRI.** Cys-Fe_3O_4 NP-labeled GL261 cells were collected in a 1.5 mL tube. The tube was placed in an MRI coil

(14) Hayashi, K.; Moriya, M.; Sakamoto, W.; Yogo, T. *Chem. Mater.* **2009**, *21*, 1318.
(15) Chikazumi, S. *Physics of Ferromagnetism*; Oxford University Press: Oxford, UK, 1997.
(16) Gerweck, L. E. *Radiat. Res.* **1977**, *70*, 224.
(17) Pankhurst, Q. A.; Connolly, J.; Jones, S. K.; Dobson, J. *J. Phys. D: Appl. Phys.* **2003**, *36*, R167.
(18) Lee, J.-H.; Huh, Y.-M.; Jun, Y.-w.; Seo, J.-w.; Jang, J.-t.; Song, H.-T.; Kim, S.; Cho, E.-J.; Yoon, H.-G.; Suh, J.-S.; Cheon, J. *Nat. Med.* **2007**, *13*, 95.
(19) Laurent, S.; Forge, D.; Port, M.; Roch, A.; Robic, C.; Elst, L. V.; Muller, R. N. *Chem. Rev.* **2008**, *108*, 2064.
(20) Tayim, H. A.; Sabri, M. *Inorg. Nucl. Chem. Lett.* **1973**, *9*, 753.
(21) Kawasaki, H.; Akira, T.; Watanabe, T.; Nozaki, K.; Yonezawa, T.; Arakawa, R. *Anal. Bioanal. Chem.* **2009**, *395*, 1423.

Scheme 1. Synthesis Procedure for Cys-Fe_3O_4 NPs

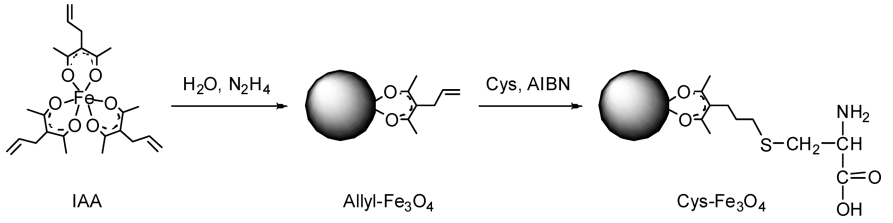

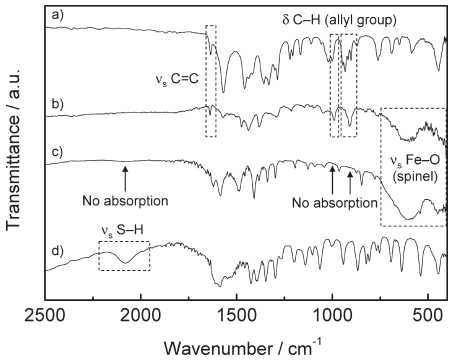

Figure 1. FTIR spectra of (a) IAA, (b) Allyl-Fe_3O_4 NPs, (c) Cys-Fe_3O_4 NPs, and (d) cysteine.

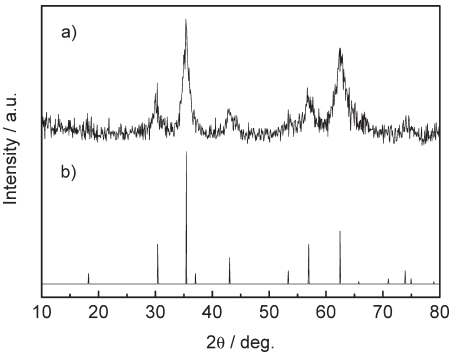

Figure 2. XRD patterns of (a) Cys-Fe_3O_4 NPs and (b) Fe_3O_4 (JCPDS No. 391346).

(MRmicro 10, MRTechnology), and the T_2-weighted images were obtained according to procedures specified by the manufacturer.

Results and Discussion

Synthesis of Cys-Fe_3O_4 NPs. Scheme 1 shows the synthesis procedure for Cys-Fe_3O_4 NPs. The synthesis was achieved by a one-pot approach: *in situ* hydrolysis−condensation of IAA for producing allyl-Fe_3O_4 NPs and the modification of allyl-Fe_3O_4 NPs with cysteine via the thiol−ene click reaction. A black solution containing allyl-Fe_3O_4 NPs was obtained by *in situ* hydrolysis−condensation of IAA. Subsequently, by simply adding cysteine and AIBN to the as-prepared allyl-Fe_3O_4 NP-dispersed ethanol solution and heating the mixture, the allyl group on the surface of Fe_3O_4 NPs was bound to the thiol group of cysteine by radical addition of thiol to alkene, resulting in the formation of Cys-Fe_3O_4 NPs.

The modification of Fe_3O_4 NPs with cysteine via the thiol−ene click reaction was confirmed by FTIR (Figure 1). IAA shows absorption bands at 1635, 998, and 950−900 cm^{-1} due to the allyl group; ν_s C=C and δ C−H (Figure 1a). In the spectrum for allyl-Fe_3O_4 NPs (Figure 1b), bands attributed to the Fe−O of a spinel structure[22] are observed at 600 cm^{-1} together with allylic absorptions. This indicates the preservation of the allyl group and the formation of spinel particles after the hydrolysis−condensation of IAA. Allyl-Fe_3O_4 NPs underwent the thiol−ene reaction with cysteine, resulting in the disappearance of the bands attributed to the allyl group as shown in Figure 1c. In addition, the band disappeared after the thiol−ene reaction as shown in Figure 1c, although the thiol-derived band, ν_s S−H, was observed for cysteine at 2080 cm^{-1} as shown in Figure 1d. The results demonstrated the formation of cysteine-bound spinel particles.

Furthermore, a mass peak was observed for cysteine-bound spinel particles at m/z 261.3, which corresponded to the molecular unit formed by the bonding between allylacetylacetone and cysteine.

The inorganic phase of cysteine-bound spinel particles was identified to be Fe_3O_4 (Figure 2) by the XRD pattern. The crystallite size estimated by the Scherrer equation was 7.4 nm. The results obtained by FTIR, MALDI-MS, and XRD support the view that the synthesis of Cys-Fe_3O_4 NPs was achieved by the combination of *in situ* hydrolysis−condensation and thiol−ene click chemistry.

Figure 3a shows Cys-Fe_3O_4 NPs dispersed in a water−chloroform solution. Cys-Fe_3O_4 NPs are uniformly dispersed in water but not chloroform. Moreover, the NPs can be easily collected by a magnet (Figure 3b). Figure 3c shows the light transmittance of Cys-Fe_3O_4 NP-dispersed water immediately after dispersion in water and a month later. As no significant change in transmittance was observed for more than a month, the NPs were stable in water for a prolonged period.

The particle diameter of Cys-Fe_3O_4 NPs estimated by TEM was ~8.0 nm (Figure 4a), which was comparable with the crystallite size calculated from XRD. The hydrodynamic diameter measured by DLS was ~22 nm (Figure 4b), which was larger than the directly observed size by TEM, because the organic molecules on the surface of the NPs swelled in water. Thus, DLS revealed the whole size including the organic phase in water, while TEM showed the size of the inorganic phase in the dry state. According to TG analysis, the organic phase of the NPs was 28.5 wt %. TEM and DLS also demonstrated

(22) Tarte, P. *Comput. Rend.* **1962**, *254*, 2008.

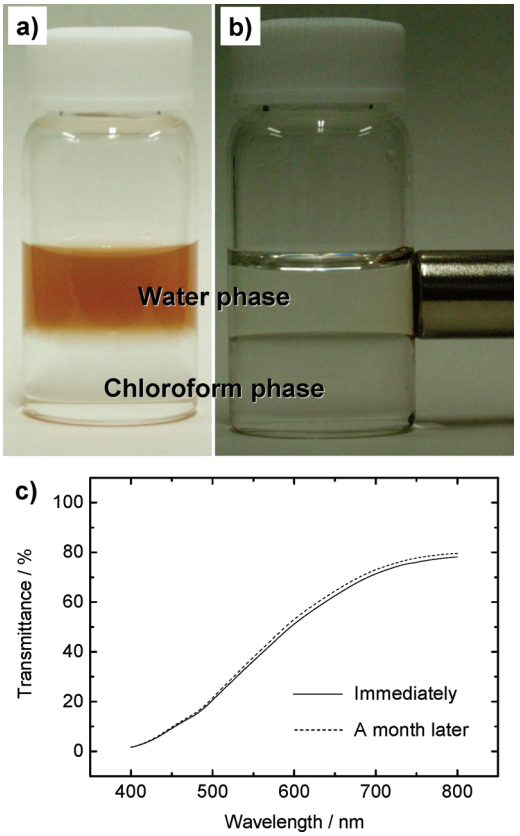

Figure 3. (a) Cys-Fe_3O_4 NP-dispersed water−chloroform solution, (b) magnetic response of Cys-Fe_3O_4 NPs dispersed in water, and (c) light transmittance change of Cys-Fe_3O_4 NP-dispersed water with the passage of time for stability test in water.

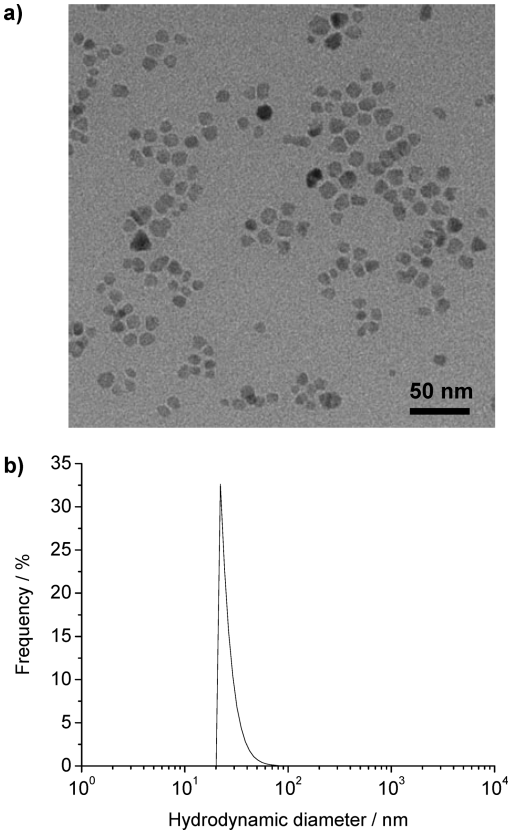

Figure 4. (a) TEM image of Cys-Fe_3O_4 NPs and (b) particle size distribution of Cys-Fe_3O_4 NPs in water by DLS.

that the NPs were monodisperse and formed no agglomerations above 70 nm, although 8.1% NPs range from 40 to 70 nm as shown in Figure 4b. Because the enhanced permeability and retention (EPR) effect, passive targeting, is applicable to NPs below 100 nm, the size of Cys-Fe_3O_4 NPs is suitable for biomedical application.[23]

Magnetic Properties of Cys-Fe_3O_4 NPs. Figure 5 shows the magnetization curve of Cys-Fe_3O_4 NPs at 300 K. The saturation magnetization was 24 emu/g. Since TG revealed the inorganic contents of Cys-Fe_3O_4 NPs to be 71.5 wt %, the corrected magnetization was found to be 34 emu/g. Both the coercivity and the remnant magnetization were zero at 300 K. Furthermore, the magnetic moment was estimated by fitting the Langevin function (eq 1) to the magnetization data:

$$M/M_S = \coth(\mu H/k_B T) - k_B T/\mu H \qquad (1)$$

where M_S is the saturation magnetization, H is the applied field, k_B is Boltzmann's constant, T is the absolute temperature, and μ is the magnetic moment. Fitting the Langevin function to the data yields $3.3 \times 10^5\ \mu_B$ for the magnetic moment of Cys-Fe_3O_4 NPs, where μ_B, the Bohr magneton, is 9.3×10^{-24} J/T. This demonstrates that the NPs are not merely paramagnetic but superparamagnetic since paramagnetic moments are generally only a few μ_B,

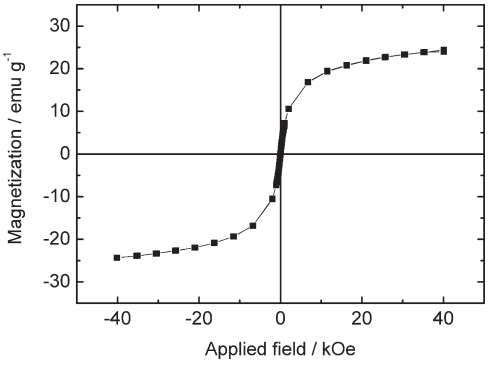

Figure 5. $M-H$ curve of Cys-Fe_3O_4 NPs at room temperature.

whereas superparamagnetic moments can be as large as $10^5\ \mu_B$.[24]

Hyperthermic Properties of Cys-Fe_3O_4 NPs. Cys-Fe_3O_4 NPs were uniformly dispersed in an agar phantom. The phantom was exposed to an AC magnetic field with a frequency of 230 kHz and an amplitude of 100 Oe: these values were within ranges harmless to the human body. The concentration of Cys-Fe_3O_4 NPs in the phantom was 10 mg/mL, which was reasonable for magnetic hyperthermia in human patients.[12] The temperature of the Cys-Fe_3O_4 NP-containing phantom increased from 37 to 42 °C, an effective temperature for hyperthermia, by applying the

(23) Nie, S.; Xing, Y.; Kim, G. J.; Simons, J. W. *Annu. Rev. Biomed. Eng*. **2007**, *9*, 257.

(24) Dennis, C. L.; Borges, R. P.; Buda, L. D.; Ebels, U.; Gregg, J. F.; Hehn, M.; Jouguelet, E.; Ounadjela, K.; Petej, I.; Prejbeanu, I. L.; Thornton, M. J. *J. Phys.: Condens. Matter*. **2002**, *14*, R1175.

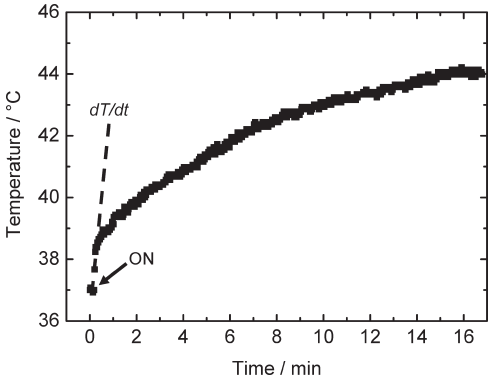

Figure 6. Temperature increase of Cys-Fe_3O_4 NPs by applying an AC magnetic field 230 kHz in frequency and 100 Oe in amplitude.

field only for 6 min (Figure 6). The temperature of the phantom increased up to 44 °C under the influence of the field for 15 min and thereafter stayed constant. The amount of heat generation was evaluated by the specific absorption rate (SAR) value. The SAR value of Cys-Fe_3O_4 NPs was calculated by the following equation:

$$\mathrm{SAR} = C(\mathrm{d}T/\mathrm{d}t)(m_a/m_m) \quad (2)$$

where C is the specific heat capacity of water (4.2 J/g·K), $\mathrm{d}T/\mathrm{d}t$ is the initial slope of the temperature versus time curve upon application of the AC magnetic field, m_a is the mass of the Cys-Fe_3O_4 NP-containing phantom, and m_m is the mass of Fe_3O_4 in the phantom.[1] The SAR value of Cys-Fe_3O_4 NPs estimated by eq 2 was 156 W/g. Hergt et al. reported that the SAR value of Endorem, an MRI contrast agent consisting of 6-nm-Fe_3O_4 NPs, was <0.1 W/g at 300 kHz and 82 Oe.[25] Timko et al. also investigated the SAR values of magnetosomes, which are Fe_3O_4 or Fe_3S_4 crystals 30−140 nm in diameter enveloped by a biological membrane including phospholipids and specific proteins. The SAR values were 171 W/g at 750 kHz and 63 Oe field amplitude and 841 W/g at 750 kHz and 126 Oe.[26] Given that the SAR value is generally proportional to the frequency and the square of the amplitude of the magnetic field,[27] the heating ability of Cys-Fe_3O_4 NPs is comparable to that of magnetosomes and far superior to that of Endorem.

Cytotoxicity Assay of Cys-Fe_3O_4 NPs. The cytotoxicity of Cys-Fe_3O_4 NPs was investigated by assessing the viability of GL261 cells after incubation for 24 h in the presence of the NPs. In addition, the number of GL261 cells cultured for 24 h was measured as a control. The numbers of viable cells grown with Cys-Fe_3O_4 NPs was about the same as that in the control (Figure 7). Thus, the NPs were nontoxic to humans.

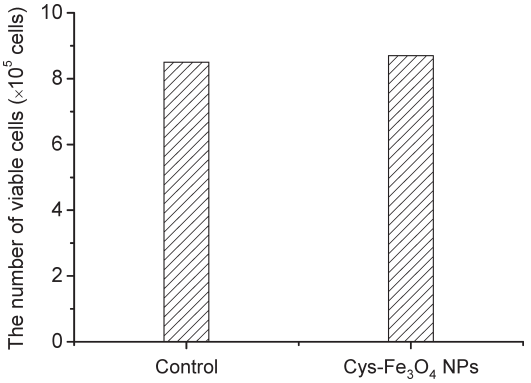

Figure 7. Cytotoxic assay of Cys-Fe_3O_4 NPs.

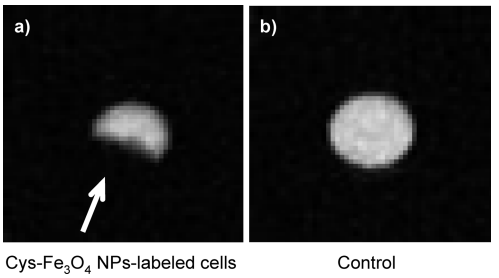

Figure 8. T_2-weighted MR images of (a) Cys-Fe_3O_4 NP-labeled cells and (b) untreated cells as the control.

MRI Contrast-Enhancing Effect of Cys-Fe_3O_4 NPs. Figure 8a shows the T_2-weighted MRI of Cys-Fe_3O_4 NP-labeled GL261 cells in a wall of the microtube. An image of untreated cells is also shown in Figure 8b as a control. A dark contrast appeared at the position indicated by the arrow in Figure 8a, while only a white image was observed in Figure 8b. The contrast was caused by a shortening of the T_2 relaxation time of the protons around Cys-Fe_3O_4 NPs.[28] This result demonstrates that Cys-Fe_3O_4 NPs can be employed as an MRI contrast agent.

Conclusions

We successfully achieved a one-pot biofunctionalization of Fe_3O_4 NPs with cysteine through the *in situ* hydrolysis−condensation of IAA followed by the thiol−ene click reaction. Biofunctionalization made Fe_3O_4 NPs hydrophilic and biocompatibile. Cys-Fe_3O_4 NPs exhibited superparamagnetism and superior hyperthermic properties. Furthermore, the NPs showed a T_2-weighted MRI contrast-enhancing effect. Therefore, the NPs can be used as heating devices for magnetic hyperthermia and as MRI contrast agents. In addition, this approach, the *in situ* hydrolysis−condensation of allyl-containing metal−organic compounds and the thiol−ene click reaction, allows one-pot biofunctionalization of inorganic NPs with thiol-containing peptides, molecules, and polymers. Thus, it is a versatile method for the surface functionalization of NPs.

(25) Hergt, R.; Andrä, W.; d'Ambly, C. G.; Hilger, I.; Kaiser, W. A.; Richter, U.; Schmidt, H.-G. *IEEE Trans. Magn.* **1998**, *34*, 3745.
(26) Timko, M.; Dzarova, A.; Kovac, J.; Skumiel, A.; Józefczak, A.; Hornowski, T.; Gojżewski, H.; Zavisova, V.; Koneracka, M.; Sprincova, A.; Strbak, O.; Kopcansky, P.; Tomasovicova, N. *J. Magn. Magn. Mater.* **2009**, *321*, 1521.
(27) Rosensweig, R. E. *J. Magn. Magn. Mater.* **2002**, *252*, 370.
(28) Cheon, J.; Lee, J.-H. *Acc. Chem. Res.* **2008**, *41*, 1630.